Journal of Environmental Economics & Chemical Processes (JEECP)

https://doi.org/10.22034/jeecp.2025.735026

Journal homepage: *WWW.JEECPJournal.com*

Journal of Environmental Economics & Chemical Processes (JEECP)

ORIGINAL RESEARCH PAPER

Investigation New Anionic Surfactant and Cationic Surfactant Effect on Relative Permeability Curves

Farhad Fallahi[a], Ghasem Zargar[a], Mohammad Ali Takasi[a], Abbas Khaksar Manshad[b*], Fatemeh Ozar Asl[a], Siamak Moradi[b]

[a] *Department of Petroleum Engineering, Ahvaz Faculty of Petroleum Engineering (AIT), Petroleum University of Technology, Ahvaz, Iran.*
[b] *Department of Petroleum Engineering, Abadan Faculty of Petroleum Engineering (AIT), Petroleum University of Technology, Abadan, Iran.*

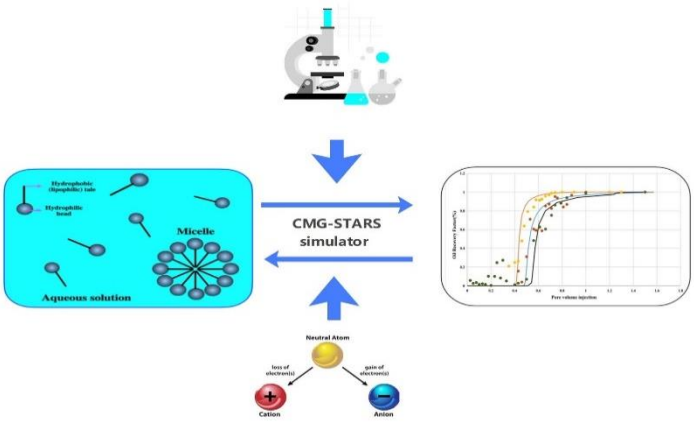
P A P E R I N F O

Paper history:
Received 10/13/2025
Accepted in revised form 12/8/2025

***Keywords*:**
Cationic surfactant
Anionic surfactant
Relative permeability
EOR, CMG software

A B S T R A C T

Surfactants have been considered as chemical EOR processes for enhanced oil recovery by reduced oil-water interfacial tension. However, these surfactants may enhance oil recovery via wettability alteration as well. Due to changes in wettability and interfacial tension, the relative permeability of oil and water and recovery of oil was changed where several fluids flow in porous media. This study investigates the effect of anionic and cationic surfactants and their effect on the wettability of sandstones in the presence of oil and water. The effect of these surfactants on the relative permeability (relative two-phase permeability) of several methods and correlations were discussed. Also, comparing the relative permeability data obtained from these methods with the relative permeability diagrams obtained from the CMG-STARS simulator (which was plotted using the Corey method) to find the method closest to the simulation curves was described. To investigate this factor, several core flood experiments were performed using the sandstone core of Bangestan oil reservoir by a core-flood apparatus. Results of this study demonstrated that the cationic Dodecyl Trimethyl Amino Bromide and anionic Dodecyl-Amino-Benzene Sulfonic Acid alter wettability of sandstone rocks to more water-wet, reduced relative permeability of water and relative permeability of oil was increased. Therefore, these surfactants enhanced recovery of oil in rocks. But the experiment show that the Dodecyl-Amino-Benzene sulfonic Acid surfactant have more effect on relative permeabilities and recovery. In addition, according to the results of Honarpour et al method, the closest method of calculating the relative permeability curves to the relative permeability curves obtained from the simulator was obtained.



1. Introduction

As it has been since the beginning of the oil industry, the energy world needs to provide more oil as an energy source. This could be done either by enhancing the oil recovery or exploring new reserves. Since most of the world's reservoirs have been explored, the need for using enhanced oil recovery methods has been increased.

In recent years, due to a combination of the world's rising energy consumption, decrease in number of remaining reserves, and low recoveries by conventional methods, the field of enhanced oil recovery has grown to become more popular [1].

Oil recovery operations traditionally have been subdivided into three stages: primary, secondary, and tertiary. Historically, these stages described the production from a reservoir in a chronological sense. It was soon learned, however, that some fields would perform better if the tertiary recovery processes were implemented before the third stage in the life of the field. The drawback to consideration of the three stages as a chronological sequence is

* Corresponding author: Abbas Khaksar Manshad
E-mail address: Khaksar@put.ac.ir
ISSN: 3116-0050
URL: https://www.jeecpjournal.com/article_735026.html

Please cite this article as: F. Fallahi, Gh. Zargar, M. A. Takasi, A. Khaksar Manshad, F. Ozar Asl, S. Moradi. *Journal of Environmental Economics & Chemical Processes (JEECP)*, 2025, 2(4), 151-159.

/© 2025 The Author(s). Published by Institute of Power, Movement, and Innovative Insight

that many reservoir production operations are not conducted in the specified manner. Because of the difficulty of chronological oil-production classification, classification based on process description is more useful and is now the generally accepted approach, although the naming of the processes still incorporates the earlier scheme based on chronology. Oil recovery processes now are classified as primary, secondary, and EOR processes [1, 2].

Primary production is ordinarily the first stage of production. It relies entirely on natural energy sources. The natural forces involved in the displacement of oil during primary production are called reservoir drives. The common reservoir drives for oil reservoirs are water drive, gas cap drive, solution or dissolved gas drive and rock and liquid expansion drive [2]. In secondary recovery, water or gas is injected to enhance oil production by improving the energy of the reservoir. Water flooding is the most common secondary recovery method in oil industry [3]. EOR was defined by Lake (1989) as "oil recovery by the injection of materials not normally present in the reservoir". Green and Willhite (1998) have divided EOR processes into 5 categories [3]. EOR processes offer prospects for ultimately producing 30-60% or more of the reservoir's OOIP. There are three major enhanced oil recovery applications: chemical flooding, gas flooding and thermal recovery. Chemical flooding uses surfactants, alkali, and/or polymers to increase oil recovery (See Figure 1). Surfactants are used to lower the oil-water interfacial tension (IFT) and modify the wettability of the reservoir rock [4].

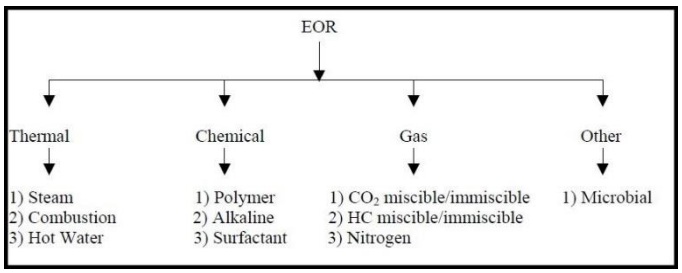


Figure 1. Flow sheet of EOR processes.

Chemical flooding relies on the addition of one or more chemical compounds to an injected fluid to reduce IFT between the reservoir oil and injected fluid [9]. Also, these chemicals make injected fluids more viscous.

Chemical processes are divided into three parts: polymer flooding, surfactant-polymer flooding, and alkaline flooding.

The polymer flooding technique involves the addition of a polymer to the injected water to increase its viscosity. A polymer solution moves in a uniform manner. Thus, the primary mechanism in a polymer flood is an increase in volumetric efficiency.

Alkaline flooding is the injection of water solutions of certain chemicals such as sodium hydroxide, sodium silicate, and sodium carbonate. When an alkaline solution is mixed with certain crude oils, surfactant molecules are formed by chemical reactions between the alkaline solution and the oil. When the formation of surfactant molecules occurs in situ, the IFT between the brine and oil phases can be significantly reduced. The reduction of IFT causes the microscopic displacement efficiency to increase.

Surfactant/polymer flooding can be any one of several processes in which detergent-like materials are injected as a slug of fluid to modify the chemical interaction of oil with its surroundings. The primary purpose of surfactant is too lower IFT. Because of the cost of such agents, to preserve the integrity of the slug it is pushed by water to which a polymer has been added. Surfactants have one part that has an affinity for nonpolar media and one part that has an affinity for polar media. These molecules form oriented monolayers at interfaces and show surface activity (i.e., they lower the surface or interfacial tension of the medium in which they are dissolved). In some usage surfactants are defined as molecules capable of associating to form micelles. Surfactants have many well-known applications in wettability alteration and interfacial tension reduction. These materials impact fluid movement and fluid saturation by affecting capillary pressure and relative permeabilities [5]. Surface active agents are amphiphilic, usually organic compounds with a chemical structure that consists of two different molecular components, known as hydrophilic and hydrophobic groups (Figure 2). A hydrophilic group is a water-soluble component. A hydrophobic group is a water-insoluble component. In the standard surfactant terminology, the soluble component, or hydrophilic group, is called the "head", and the hydrophobic group is called the "tail". The head and tail surfactants attack the interface between two immiscible surfaces, thus decreasing the interfacial forces between the two surfaces. Surfactants have different types: Anionic, Nonionic, Cationic, and Amphoteric surfactants (Figure 3).

Anionic surfactants are the most commonly-used surfactants. They dissociate in water into an amphiphilic anion and a cation which is in general alkaline metal (Na^+, K^+) or a quaternary ammonium. They include alkylbenzene sulfonates detergents, fatty acid soaps, lauryl sulfate foaming agent, di-alkyl sulfosuccinate wetting agent, and lignosulfonates dispersants.

Nonionic surfactants are the second most commonly-used surfactants. They do not ionize in aqueous solution, because their hydrophilic group is of a non-dissociable type, such as alcohol, phenol, ether, ester, or amide. A large proportion of these nonionic surfactants are made hydrophilic by the presence of a polyethylene glycol chain, obtained by the polycondensation of ethylene oxide. As a consequence, they are compatible with other types and are excellent candidates to enter complex mixtures, as found in many commercial products. They are much less sensitive to electrolytes, particularly divalent cations, than ionic surfactants, and can be used with high salinity or hard water.

Cationic surfactants are dissociated in water into an amphiphilic cation and an anion, most often of the halogen type. A very large proportion of this class corresponds to nitrogen compounds such as fatty amine salts and quaternary ammoniums, with one or several long chain of the alkyl type, often coming from natural fatty acids. These surfactants are in general more expensive than anionics, because of the high-pressure hydrogenation reaction to be carried out during their synthesis. As a consequence, they are only used in two cases in which there is no cheaper substitute, i.e., a) as bactericide, b) as positively charged substance which is able to adsorb on negatively charged substrates to produce antistatic and hydrophobant effect, often of great commercial importance such as in corrosion inhibition.

When a single surfactant molecule exhibit both anionic and cationic dissociations it is called amphoteric or zwitterionic. This is the case of synthetic products like betaines or sulfobetaines and natural substances such as aminoacids and phospholipids. Some amphoteric surfactants are insensitive to pH, whereas others are cationic at low pH and anionic at high pH, with an amphoteric behavior at intermediate pH. Amphoteric surfactants are generally quite expensive, and consequently, their use is limited to very special applications such as cosmetics where their high biological compatibility and low toxicity is of primary importance.

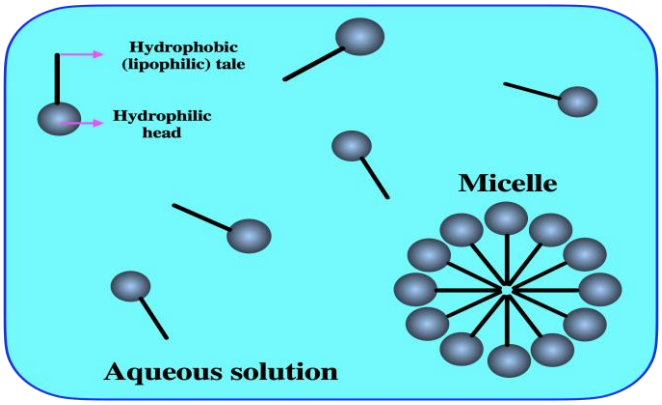


Figure 2. Surfactant chemical structure.

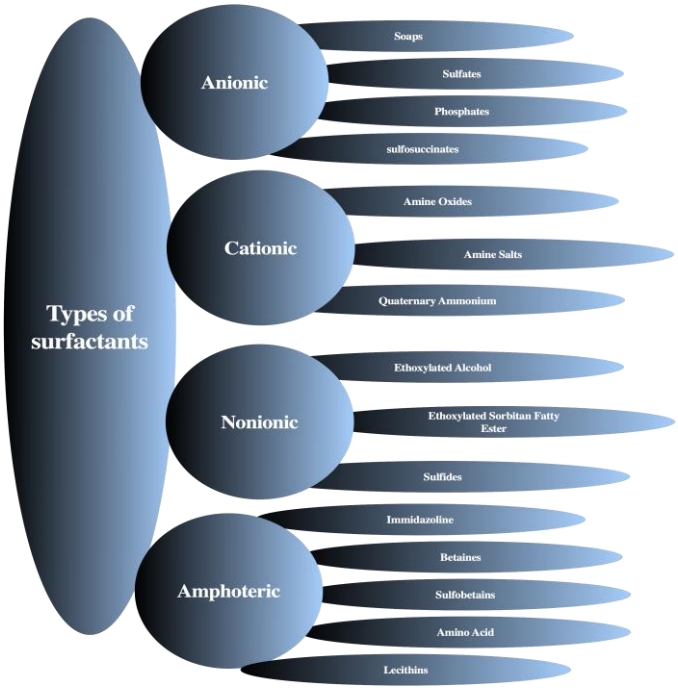


Figure 3. Classification of surfactants.

Improve the recovery of hydrocarbon reservoirs is one of the important challenges facing the petroleum engineers. Recovery mechanisms at the porous media such as water or surfactant flooding could effect on reservoir rock wettability and relative permeability. Therefore, understanding of several flooding and their influences on rock wettability and permeability can help us to optimize the oil recovery operation [6].

Relative permeability is an essential petrophysical data required for characterization of multiphase flow in petroleum reservoirs. Frequently, the relative permeability data of the two-phase flow in porous media is determined by interpreting the data of the laboratory displacement tests carried out with cylindrical core plugs extracted from petroleum reservoirs. The Darcy law and the material balance equations, with appropriate initial and boundary conditions, are applied to describe the flow of the various fluid phases in porous media [7].

An attempt is made in this project to investigate the effect of surfactants on enhanced oil recovery and its effect on relative permeability of oil and water. The use of surfactants has long been considered in oil industry for enhanced oil recovery through reduction in oil-water interfacial tension.

The purpose of this work is to investigate the performance of cationic and anionic surfactants on the relative permeability curves and oil recovery of the sandstone sample from experimental studies and comparison of results with CMG-STARS simulator. The present study is divided to two main sections:

1. Investigation of relative permeability and oil recovery of two surfactant injection and compare with water injection.

2. Comparison of the results obtained by drawing the relative permeability curves of 6 methods include Honarpour et al., Capillary data correlation, analytical correlation, Alternate method, Jones and Roszelle method, and JBN method with the relative permeability curves (Corey method) obtained from the CMG-STARS simulator to obtain the closest method to the simulated model. Figure 4 shows the flow chart of this study.

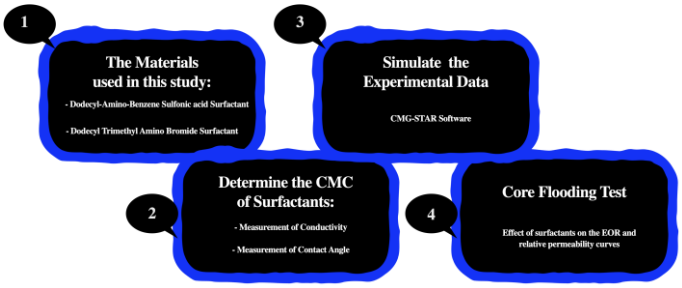


Figure 4. experimental and simulation flow chart.

2. Materials and Method

2.1. Core Samples

Cemented fine-grained sandstone core is used in our experiments. The absolute permeability of the sample was obtained from core flood apparatus as 876 mD. A core plug was cut from main core sample. The core plug diameter and length were 3.8 and 15 cm at all experiments. The porosity of the core plug is the 23%.

2.2. Oil Phase

Crude oil used in this study was provided from Iranian oil reservoir namely Bangestan formation. The composition and analysis of the crude oils is presented in Table 1 and 2. The asphaltene content in oil was 8.5 percent and viscosity of the oil used in 20ºC is 11.5 cp. The crude oil under study was relatively heavy tank oil with 24.46°API.

Table 1. Composition of crude oil sample.

Composition	Reservoir Oil (moil %)
H_2S	1.39
N_2	0.88
CO_2	5.18
C_1	22.57
C_2	6.94
C_3	5.91
iC_4	0.98
nC_4	2.97
C_5^+	53.9

Table 2. Physical properties.

Molecular weight of reservoir oil	1.38
Sp. Gr.@ 60/60 ^{0}F	0.9355
Density @ reservoir pressure (g/cc)	0.7577
API gravity	24.46
Oil viscosity @ reservoir pressure (cp)	1.3170
Reservoir pressure (psia)	5684
Reservoir temperature (^{0}F)	255

2.3. Surfactants

Two different surfactants are used in this experimental study are "Dodecyl-Amino-Benzene Sulfonic acid" and "Dodecyl Trimethyl Amino Bromide".

2.4. CMC Measurement

The behavior of surfactants is determined by their concentration in the bulk solution. when surfactant concentration increases the number of surfactant molecules adsorbed to the interface rises, causing the surface tension to fall in a concentration dependent manner. There is a limit to the number of surfactant molecules that can absorb to a surface before that surface becomes fully covered or saturated, leaving no ‘room‘for further surfactant molecules to align themselves across the surface. The surfactant concentration at which this occurs is termed the critical micelle concentration (CMC).

In polar solvents such as water, amphiphilic surfactant monomers assemble to form a micelle in such a way that their hydrocarbon tails huddle in the core of the micelle, and the polar head group project outwards into the polar bulk solution and locate at the micelle-water interface such that the hydrophobic tails are shielded from water. Micelles often drawn as static structures of spherical aggregates of oriented surfactant molecules. However, micelles are in dynamic equilibrium with surfactant monomers in the bulk, which are frequently being exchanged with the surfactant molecule in the micelles. The equilibrium between monomer and aggregate is established within a few milliseconds. At equilibrium, the number of micelles disintegrated in the same time.

There are many ways in which CMC could be determined. The CMC is the narrow concentration range over which amphiphilic or surfactant solutions show an abrupt change in a physical property such as electrical conductivity, surface tension, osmotic pressure, density. Light scattering or refractive index.

The conductance of a solution, can give important quantitative information regarding the ionic composition of a sample. Conductance is a measure of a sample’s ability to pass a current and strongly depends on the concentration, mobility, and charge of ions in solution.

2.5. Measurement of Wettability Alteration

Distilled water is used as the aqueous phase for contact angle, flooding tests and solutions. One of the best wettability measurement methods when pure fluids and artificial cores are used is the contact angle. Several core slices called “pellet” with 1cm diameter are used in contact angle test. These samples are aged in oil for 48 hours and then aged in different surfactants and water for 8 hours.

In the sessile drop method, the flat surface of pellet is suspended horizontally in the oil (kerosene) and placed a drop of water on the surface of the pellet (see figure 3-6). Then the contact angle between water drop, slice surface and oil is measured. When θ is between 0° and 60° to 75° in such a system, it is defined

as water-wet. When θ is between 105° to 120° and 180° the system is defined as oil-wet. In the range of a 75° to 105° contact angle, the system is neutral-wet.



Figure 1. Contact angle measurement.

2.6. Core Flooding Experimental Set-Up and Process

After preparing, cleaning the core sample and core specification determination, it is saturated with distilled water by vacuumed pump. Then the core is placed in the rubber sleeve in the core holder. This sleeve is used as a connection to exert overburden pressure on the rock. In these experiments the overburden pressure is provided by water (2500 psi). To reach S_{wi}, injection of oil is continued until no water is detected at the outlet. Volume of discharged water is measured and the S_{wi} is calculated. A Schematic of Core flood experimental setup is illustrated in Figure 5.

Now to reach residual oil saturation Sor, distilled water is injected into the core plug at constant flow rate of 1 ml/min until no oil is produced at the outlet. Difference between injected oil volume and produced oil divided to total pore volume indicates residual oil saturation, S_{or}.

Then the core was saturated with oil again and core sample is flooded with water. In each one minutes the oil and water volume produced was measured and the difference pressure that show in apparatus was observed to calculate the oil recovery and relative permeabilities.

This step is repeated with two surfactants at CMC concentration. The relative permeability curves and recovery was measured and plotted by several methods.

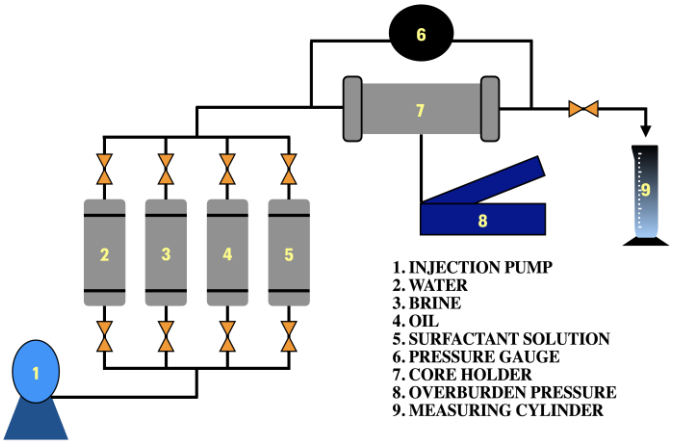


Figure 5. Schematic of core flood experimental setup.

2.7. Two-phase Relative Permeability Measurements

In many cases, relative permeability data on actual samples from the reservoir under study may not be available, in which case it is necessary to obtain the desired relative permeability data in some other manner. Field relative permeability data can usually be calculated. The field data are unavailable for future production, however, and some substitute must be devised. Several methods have been developed for calculating relative permeability relationships. Various parameters have been used to calculate the relative permeability relationships, including [6]:

- Residual and initial saturations
- Capillary pressure data

In addition, most of the proposed correlations use the effective phase saturation as a correlating parameter. The effective phase saturation is defined by the following set of relationships [6]:

$$S_o^* = \frac{S_o}{1-S_{wc}} \quad (1)$$

$$S_w^* = \frac{S_w - S_{wc}}{1-S_{wc}} \quad (2)$$

$$S_g^* = \frac{S_g}{1-S_{wc}} \quad (3)$$

Where:

S_o^*, S_w^*, S_g^*= effective oil, water and gas saturation, respectively
S_o, S_w, S_g= oil, water and gas saturation respectively
S_{wc} = Connate (irreducible) water saturation

2.7.1. Relative Permeability from Honarpour et al. Correlation

Knop developed a correlation from 107 experimentally determined gas-oil relative permeability ratios of Venezuelan core samples. The core samples were from consolidated as well as poorly consolidated sandstone reservoirs of high porosity and permeability; the Welge gas-flood procedure was used for krg/kro determination. A single correlation was established based on the restored-state water saturation as a correlating parameter. Comparison of Knopp's correlation with experimental values is more promising when the geometric mean of the suite of krg/kro curves for a given reservoir or sample group is compared with the corresponding most probable curves for the correlation. Knopp also suggested a procedure for developing similar correlations for various other formations. Honarpour et al. developed asset of empirical prediction equations for water-oil imbibition relative permeability and gas-oil drainage relative permeability from a large number of experimental data. Their results are presented as:

Water wet system:

$$k_{rw} = 0.035388\left(\frac{S_w - S_{wi}}{1-S_{wi}-S_{orw}}\right) - 0.010784\left(\frac{S_w - S_{orw}}{1-S_{wi}-S_{orw}}\right)^{2.9} + 0.56556\,S_w{}^{3.6}(S_w - S_{wi}) \quad (4)$$

Intermediately wet system:

$$k_{rw} = 1.5814\left(\frac{S_w - S_{wi}}{1-S_{wi}}\right)^{1.91} - 0.58617\left(\frac{S_w - S_{orw}}{1-S_{wi}-S_{orw}}\right)(S_w - S_{wi}) - 1.2484\emptyset(1-S_{wi})(S_w - S_{wi}) \quad (5)$$

Any wettability system:

$$k_{ro,w} = \left(\frac{\frac{S_o}{1-S_{wi}} - S_{or}}{1-S_{orw}}\right)^{1.8}\left(\frac{S_o - S_{orw}}{1-S_{wi}-S_{orw}}\right)^2 + 2.6318\emptyset(1-S_{orw})(S_o - S_{orw}) \quad (6)$$

Any wettability system:

$$k_{ro,g} = 0.98372\left(\frac{S_o}{1-S_{wi}}\right)^4\left(\frac{S_o - S_{org}}{1-S_{wi}-S_{org}}\right)^2 \quad (7)$$

Any wettability system

$$k_{rg} = 1.1072\left(\frac{S_g - S_{gc}}{1-S_{wi}}\right)^2 k_{rg(S_{org})} + 2.7794\left(\frac{S_{org}(S_g - S_{gc})}{1-S_{wi}}\right)k_{rg(S_{org})} \quad (8)$$

2.7.2. Relative Permeability from Capillary Pressure Data

Rose and Bruce (1949) showed that capillary pressure pc is a measure of the fundamental characteristics of the formation and could also be used to predict the relative permeabilities. Based on the concepts of tortuosity, Wyllie and Gardner (1958) developed the following mathematical expression for determining the drainage water-oil relative permeability from capillary pressure data [6]:

$$P_c = 22 - 20S_w \quad (9)$$

$$K_{rw} = \left(\frac{S_w - S_{wc}}{1-S_{wc}}\right)^2 \frac{\int_{S_{wc}}^{S_w} \frac{dS_w}{p_c^2}}{\int_{S_{wc}}^{1} \frac{dS_w}{p_c^2}} \quad (10)$$

$$K_{ro} = \left(\frac{1-S_w}{1-S_{wc}}\right)^2 \frac{\int_{S_w}^{1} \frac{dS_w}{p_c^2}}{\int_{S_{wc}}^{1} \frac{dS_w}{p_c^2}} \quad (11)$$

Wyllie and Gardner also presented two expressions for generating the oil and gas relative permeabilities in the presence of the connate water saturation. The authors considered the connate water as part of the rock matrix to give [6]:

$$K_{ro} = \left(\frac{S_o - S_{or}}{1-S_{or}}\right)^2 \frac{\int_0^{S_o} \frac{dS_o}{p_c^2}}{\int_0^{1} \frac{dS_o}{p_c^2}} \quad (12)$$

$$K_{ro} = \left(1 - \frac{S_o - S_{or}}{S_g - S_{gc}}\right)^2 \frac{\int_0^{S_o} \frac{dS_o}{p_c^2}}{\int_0^1 \frac{dS_o}{p_c^2}} \quad (13)$$

Integrate the capillary pressure from Equation 9 in K_{ri} (i=o, w and g), to give:

$$I = \int_a^b \frac{dS_w}{(22-20S_w)^2} = \left(\frac{1}{440-400b}\right) - \left(\frac{1}{440-400a}\right) \quad (14)$$

2.7.3. Relative Permeability from Analytical Equations

Analytical representations for individual-phase relative permeabilities are commonly used in numerical simulators. The most frequently used functional forms for expressing the relative permeability and capillary pressure data are given below [6]:

2.7.3.1. Oil-Water Systems

$$k_{ro} = (K_{ro})_{S_{wc}} \left(\frac{1-S_w-S_{orw}}{1-S_{wc}-S_{orw}}\right)^{n_o} \quad (15)$$

$$k_{rw} = (K_{rw})_{S_{orw}} \left(\frac{S_w-S_{wc}}{1-S_{wc}-S_{orw}}\right)^{n_w} \quad (16)$$

2.7.3.2. Gas-Oil Systems

$$k_{ro} = (K_{ro})_{S_{gc}} \left(\frac{1-S_g-S_{lc}}{1-S_{gc}-S_{lc}}\right)^{n_{go}} \quad (17)$$

$$k_{rg} = (K_{rg})_{S_{wc}} \left(\frac{S_g-S_{gc}}{1-S_{gc}-S_{lc}}\right)^{n_g} \quad (18)$$

With:

$$S_{lc} = S_{wc} + S_{org} \quad (19)$$

Where:

S_{lc}= total critical liquid saturation
$(K_{ro})_{S_{wc}}$= oil relative permeability at connate water saturation
$(K_{ro})_{S_{gc}}$= oil relative permeability at critical gas saturation
S_{orw}= residual oil saturation in the water-oil system
S_{org}= residual oil saturation in the gas-oil system
S_{gc}= critical gas saturation
$(K_{rw})_{S_{orw}}$= water relative permeability at the residual oil saturation

n_o, n_w, n_g, n_{go}= exponents on relative permeability curves

2.7.4. Relative Permeability from Jones and Roszelle Method

Jones and Roszelle developed a graphical technique for evaluation of individual phase relative permeabilities from displacement experimental data which are linearly scalable, ignoring gravity effects and capillary pressure, water and oil relative permeabilities (expressed as functions of saturation). In this method to use the equations, the fractional flow of water or oil and effective viscosity (λ_2^{-1}), must be determined as functions of saturation then:

$$k_{rw} = {\mu_w f_w}/{\lambda_2^{-1}} \quad (20)$$

And

$$k_{ro} = {\mu_o f_o}/{\lambda_2^{-1}} \quad (21)$$

2.7.5. Relative Permeability from JBN Method

The JBN (Johnson, Bossler, and Neumann) method is a standard and unsteady-state method for determining the relative permeability curves across a range of saturation Which was suggested based on the Buckley-Lowret fluid flow model. The steps of calculating the water and oil relative permeability by using the core flooding data to the JBN method is as follows: The water fractional flow (f_w) is a parameter that is obtained by dividing the amount of water produced by the total amount of water and oil produced from the end of the core. By subtracting the water fractional flow value from 1, the oil fractional flow (f_O)value is obtained.

$$f_w = \frac{q_w}{q_o+q_w} = \frac{\frac{k_{rw}}{\mu_w}}{\frac{k_{rw}}{\mu_w}+\frac{k_{ro}}{\mu_o}} = \frac{1}{1+\frac{k_{ro}\mu_w}{k_{rw}\mu_o}} \quad (22)$$

$$f_o = 1 - f_w \quad (23)$$

Where K_{rw} is water relative permeability, μ_w is water viscosity, Kro is oil relative permeability, and μ_o is oil viscosity. likewise, can be written the formula 7 as:

$$\frac{k_{ro}\mu_w}{k_{rw}\mu_o} = \frac{1-f_w}{f_w} = \frac{f_o}{f_w} \quad (24)$$

According to the JBN method, the relative permeability values depend on the fluid saturation values. Therefore, the water saturation output from the core may be obtained from the following equation:

$$S_{we} = S_{Wavg} - t_D f_o \quad (25)$$

Where S_{we} is water saturation at the core output, S_{Wavg} is the average water saturation at the rock, t_D is the volume of water injected relative to the pore volume, and f_o is the oil fractional flow. To calculate the S_{Wavg} and t_D we use the following formulae, respectively:

$$S_{Wavg} = S_{wi} + \frac{N_p}{V_p} \quad (26)$$

$$t_D = \frac{q\,t}{\varphi\,A\,L} \quad (27)$$

Where q is the evacuation of water injection, t is the spent time, ∅ is porosity, A is the cross-section of the sample and L is the sample length.

The following formula is used to obtain the injectivity ratio:

$$I_R = \frac{\frac{q}{\Delta p}}{\left(\frac{q}{\Delta p}\right)_i} \quad (28)$$

by using this relationship, we can obtain the oil relative permeability:

$$K_{ro} = \frac{f_o}{\frac{d\left(\frac{1}{t_D I_R}\right)}{d\left(\frac{1}{t_D}\right)}} \quad (29)$$

Water relative permeability (k_{rw}) can be calculated by using the k_{ro} obtained from the above formula:

$$K_{rw} = \frac{f_w}{f_o}\frac{\mu_w}{\mu_o}K_{ro} \quad (30)$$

2.8. Simulation Methodology

Various mercantile reservoir simulators are used for modeling the complicated chemical EOR processes. The STARS module (Steam, Thermal, and Advanced Processes Reservoir Simulator) is a mercantile simulator by CMG (Computer Modelling Group) that can simulate and model intricate and advanced recovery techniques involving chemicals' injection solvents and steam. In addition, a limited difference numerical simulator unravels a collection of conservation equations. To simulate the core flooding, we need to build a model that perfectly represents the fluids in the core, the core, and the movement of fluids in the pores of the core. The data expressing the essential properties of the model are classified into divisions such as fluid data, rock data, rock-fluid interaction data, initial conditions, and well data. The core flooding tests were simulated utilizing the 3-D Cartesian model. The Corey equations are used to plot the relative permeability curves in the CMG simulator. Corey (1954) proposed a simple mathematical expression for generating the relative permeability data of the gas-oil system. Equations (31) and (32) are the Corey equations for obtaining the water and oil relative permeability:

$$K_{rw} = K_{rwiro} * \left(\frac{(S_W-S_{wcirt})}{(1-S_{wcrit}-S_{oir})^{N_W}}\right) \quad (31)$$

$$K_{row} = K_{rocw} * \left(\frac{(S_o-S_{orw})}{(1-S_{wcrit}-S_{oir})^{N_O}}\right) \quad (32)$$

3. Results and Discussion

3.1. Determination of CMC

In this step the CMC of two surfactants were measured by conductivity meter. As shown in Figures 6 and 7 the slopes of the lines in plots have an inflection point that indicate the CMC. The results of CMC are shown in Table 3.

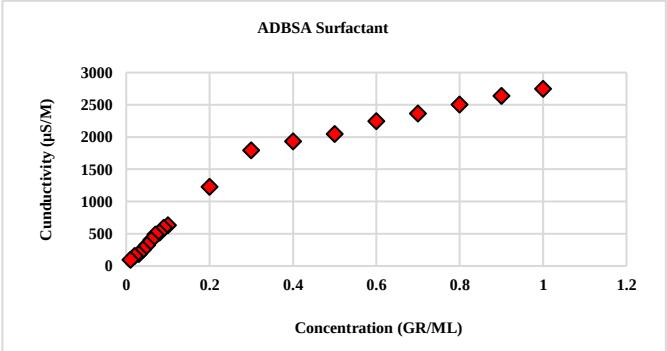


Figure 6. The graph of conductivity versus concentration of ADBSA.

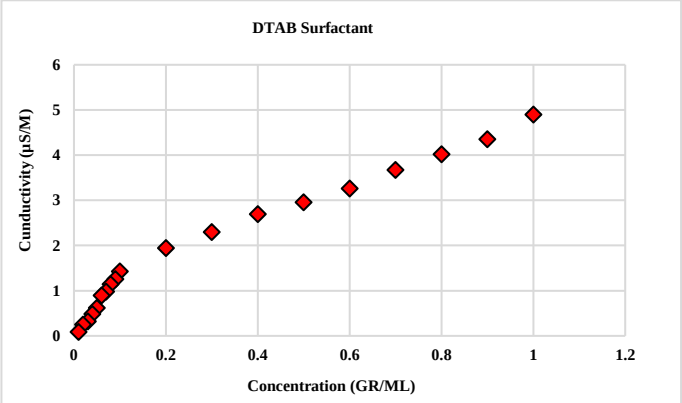


Figure 7. The graph of conductivity versus concentration of DTAB.

Table 3. CMC of the surfactants.

Surfactant	CMC (gr/ml)
Dodecyl Trimethyl Amino Bromide	0.1
Dodecyl Amino Benzene Sulfonic Acid	0.3

3.2. Contact Angle Measurement

As mentioned in prior section the contact angle method was used for measuring wettability. We done three tests, pellet aged in water and pellet aged in DTAB surfactant and ADBSA surfactant. In each test we measured the contact angle between water drop and surface of the rock. In water aging the contact angle between the pellet and water drop was 150 degrees, but in DTAB aging the contact angle was 87 degrees. Finally, when the sample was aged in ADBSA surfactant, the contact angle between the rock and water drop was 60 degrees. These tests show that when surfactant was used, the system moved to water wet. The shape of contact angle in each fluid has shown in Figure 8.

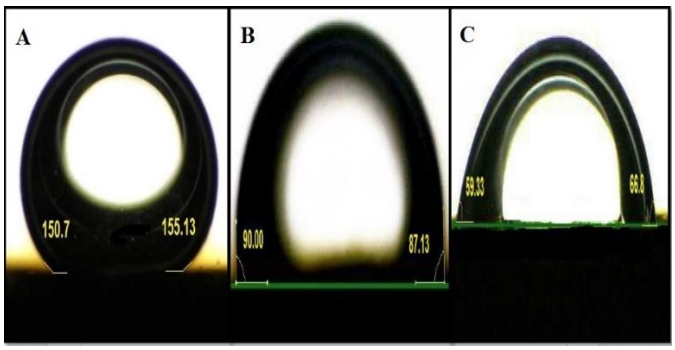


Figure 8. Contact angle between surface of the rock and water drop when the pellet was aged in: A) water, B) DTAB, C) ADBSA.

Table 4. The contact angle between surface of the rock and water drops.

Water/Surfactants	Degree(θ)
Water	150
DTAB	87
ADBSA	60

3.3. Core Flooding

3.3.1. Measurement of Porosity of Core

Before saturating the core, it was dried to a constant weight. Diameter, length and weight were measured. Then it was saturated by vacuumed pump, the saturating fluid was distilled water. When the core was completely filled with distilled water, weight of wet core was measured. Diameter of core was 3.80 cm and length was 15.0 cm then the bulk volume was 170.03cm^3. Then the following calculations were made.

• Pore volume = **(**wet weight – dry weight) / density of fluid
• Bulk volume = Area of core * length of core

• Porosity = $\frac{\text{Pore volume}}{\text{bulk volume}}$
Total pore volume = 39.12 cc
Bulk volume = 170.03
Porosity = 23%

3.3.2. Measurement of Absolute Permeability of Core

For measuring absolute permeability by injecting water at various flow rates, pressure drops are recorded. Absolute permeability of core was calculated from the slope (m) of flow rate versus pressure drop plot (Figure 9).

Absolute permeability is obtained from the following formula:

$k_{abs} = \frac{\mu l}{mA}$

The calculated permeability from Darcy equation for core, recorded rate and differential pressure are given in Table 5.

Table 5. Permeability values of core plug.

Δp (psi)	Δp (am)	Q (ml/min)	Q (cc/min)
2.9	0.1972	5	0.0833
4.8	0.3265	10	0.1666
6.6	0.4489	15	0.25
8.5	0.5782	20	0.3333

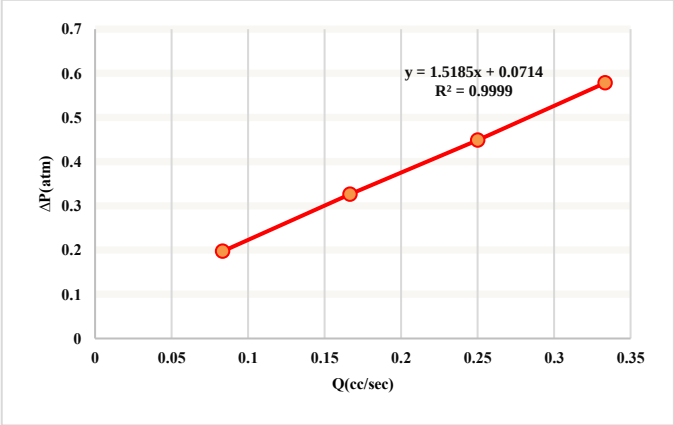


Figure 9. Differential pressure versus injection.

3.3.3. Oil Recovery Measurement

Oil recovery curve vs. pore volume injected during three injection tests in the laboratory. The amount of oil recovery in water injection was 59%, in DTAB injection recovery was 74% and in ADBSA injection the amount of oil recovery was 80%.

3.3.4. Relative Permeability

In these tests, the two-phase relative permeability (kro & krw) was measured with some methods and correlations, the results of these tests show as follows. These tests were done in unsteady state method.

The calculation to finding relative permeability of oil and water in each correlation and methods was done.

The following figures are relative permeability curves in:

- ❖ Honarpour et al. correlation
- ❖ Capillary Correlation
- ❖ Analytical equation
- ❖ Alternate Method
- ❖ Jones and Roszelle Method
- ❖ JBN Method
- ❖ Corey Method (simulation output)

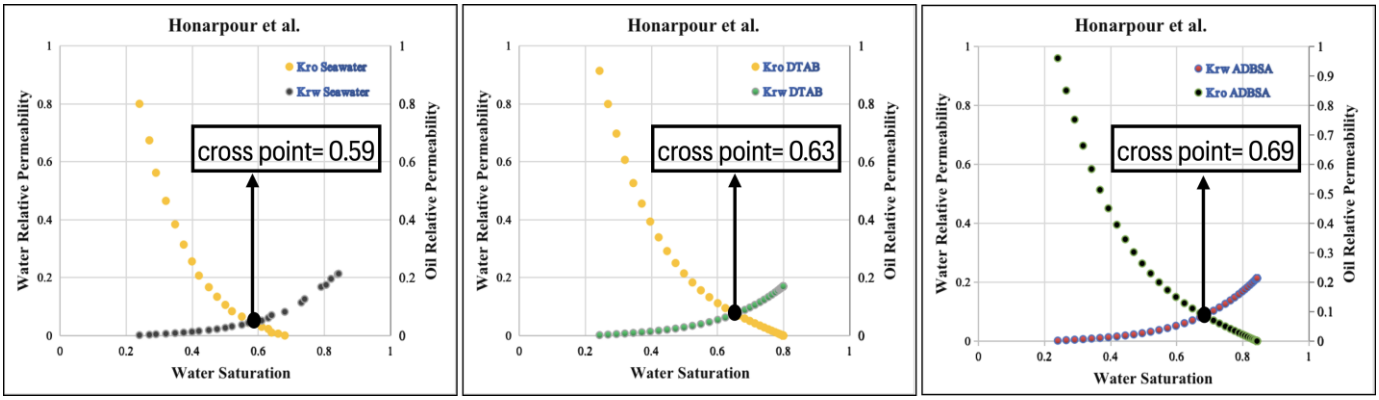


Figure 10. Oil-water relative permeability in three injection tests determined by Honarpour et al. correlation.

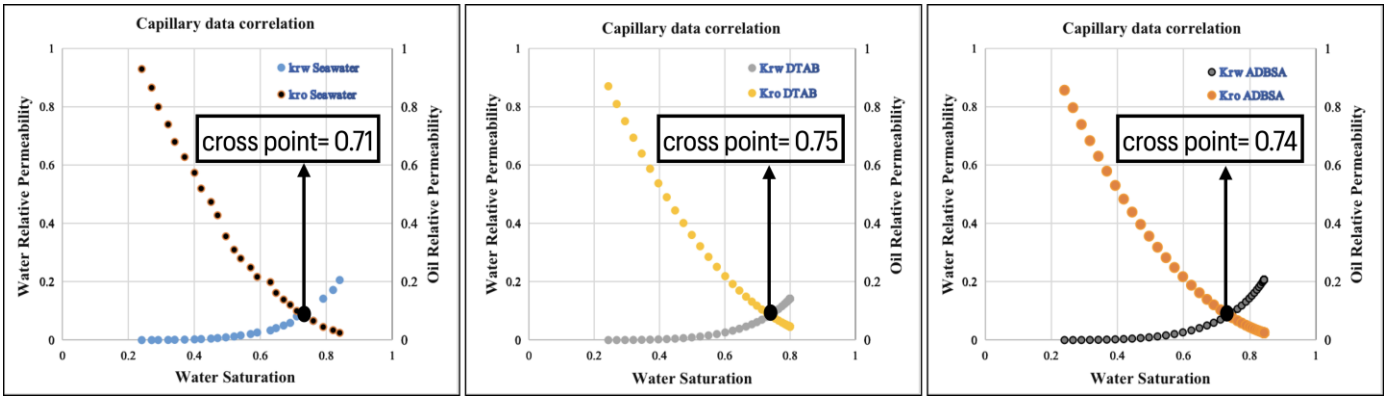


Figure 11. Oil-water relative permeability in three injection tests determined by Capillary data correlation.

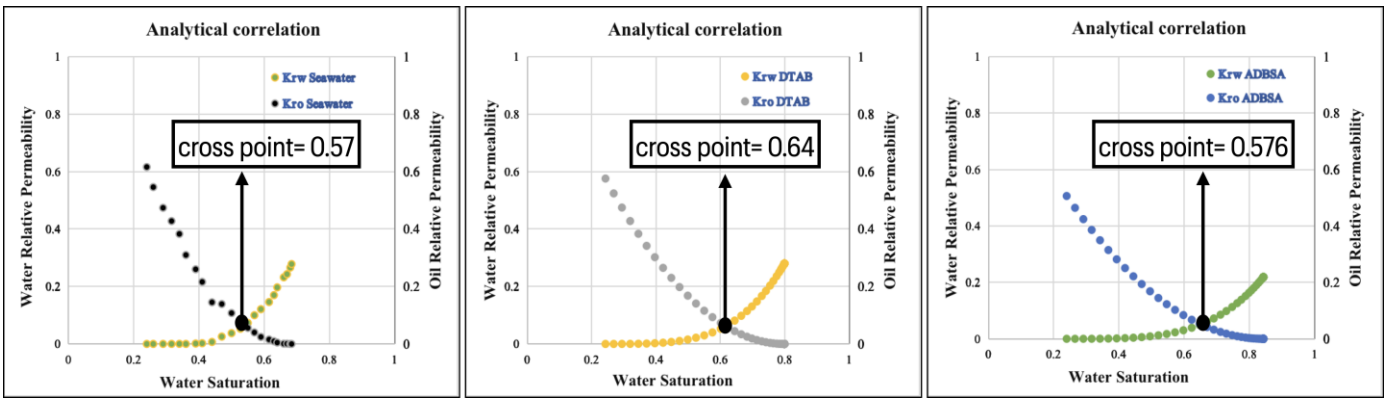


Figure 12. Oil-water relative permeability in three injection tests determined by Analytical correlation.

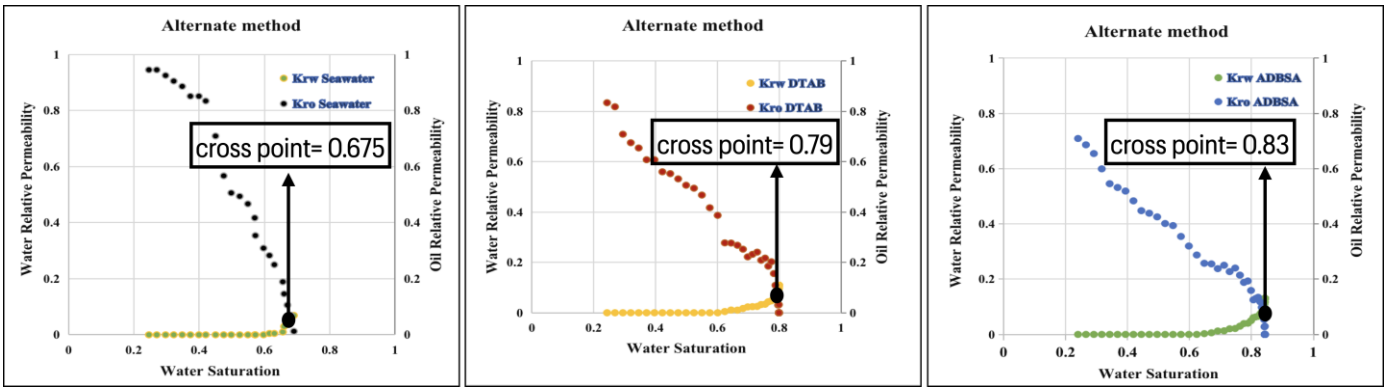


Figure 13. Oil-water relative permeability in three injection tests determined by alternate method.

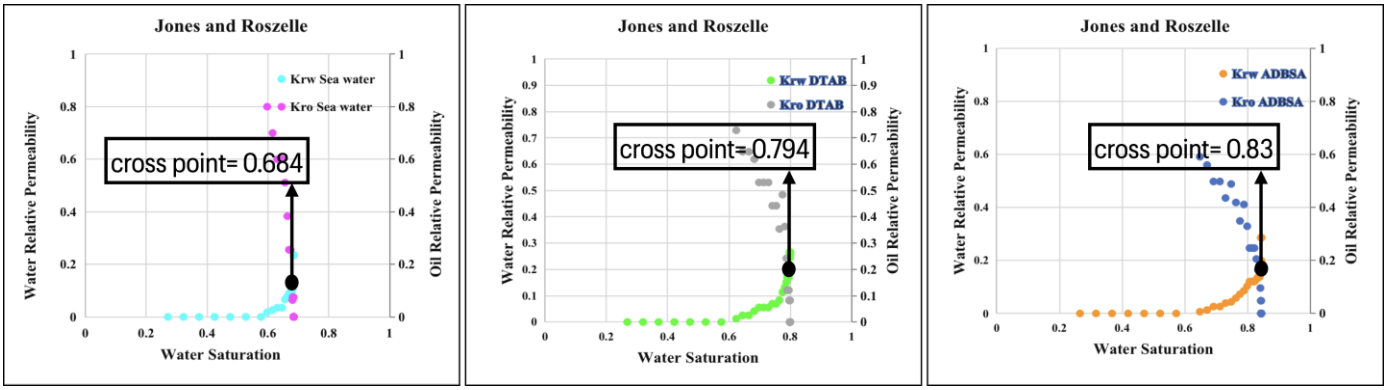


Figure 14. Oil-water relative permeability in three injection tests determined by Jones and Roszelle method.

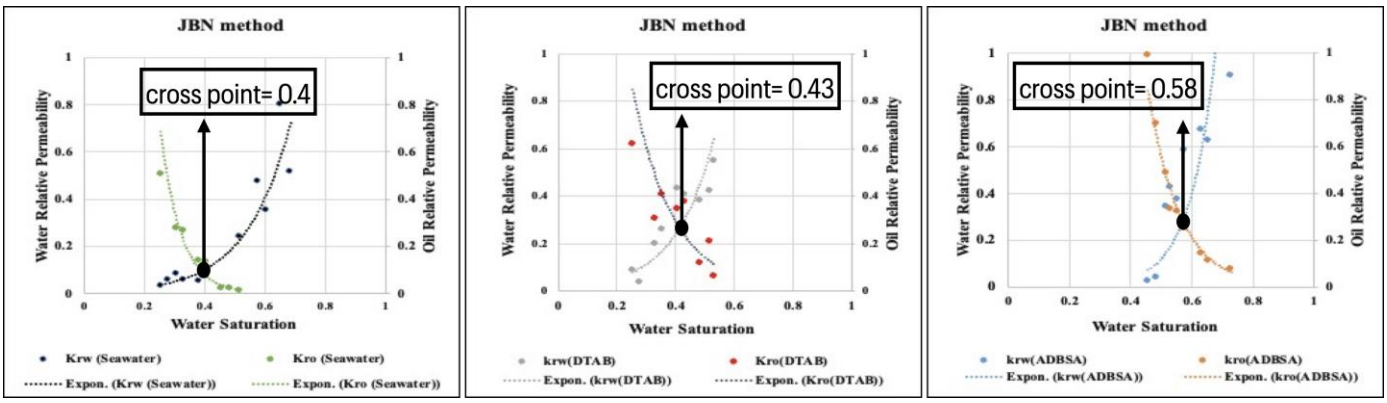


Figure 15. Oil-water relative permeability in three injection tests determined by JBN method.

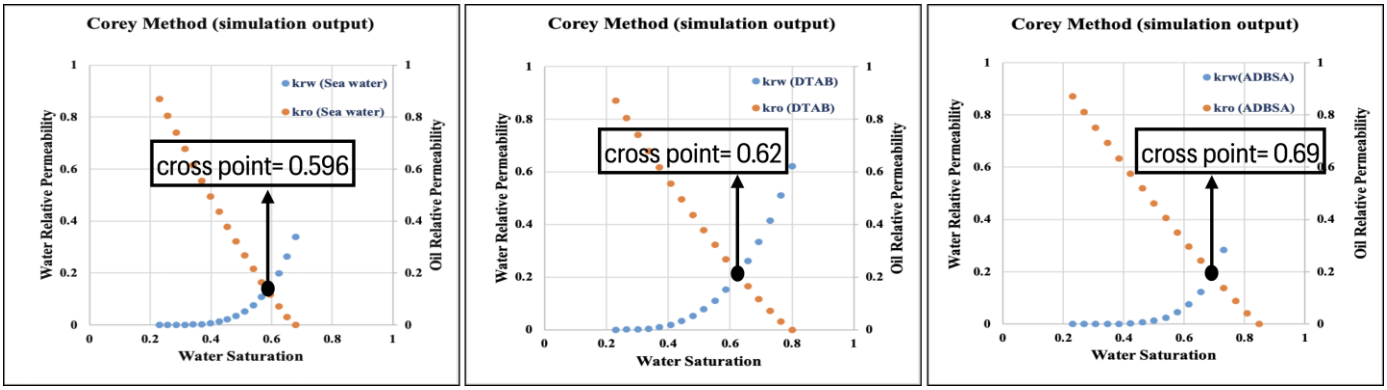


Figure 16. Oil-water relative permeability in three injection tests determined by Corey Method (simulation output) method.

The above charts show the relative permeability curves in three flooding injection. In each chart there are water injection, DTAB injection and ADBSA injection.

As shown in charts and "Jones and Roszell" method when water is injected, the cross point of water and oil relative permeabilities is in saturation of 67%. But when DTAB is injected, the cross point moves to saturation of 78%. In ADBSA injection the cross point was at the saturation of 83% that show when the surfactant is injected the core sample was more water-wet and oil moves in the core easier and faster. Also, in all charts and methods the relative permeability of water in ADBSA injection is less than DTAB injection and less than water injection. As well as the relative permeability of oil in ADBSA injection is greater than DTAB injection and water injection.

Thus, in all methods and charts when the surfactant is injected the cross point of oil and water relative permeability move to greater saturation. And in surfactant injection the relative permeability of oil increases in relative to water injection.

3.4. Model Validation Through History Matching with CMG STARS Software

We simulated a model with several 10*5*1 grids with original core dimensions in CMG software of module STARS. This model has an injection well (in 1 1 1 grid) and a production well (in 10 5 1 grid). The size of each grad is 0.67 cm in the direction of I, 3.36 cm in the direction of K and J, and the total volume of the model is equal to the original sample. Figure 17 shows the 3-dimensional Cartesian model of the Core. Before starting the flooding in the model, this model has the same irreducible water saturation in all grades. Water flooding and surfactants flooding results (liquid production rate, water cut, oil cut, and oil recovery factor) were histories matched by changing oil-water relative permeability curves and maintaining the actual rock properties such as absolute permeability and porosity (see Figure 18).

Modifying the relative permeability curves was essential to achieve a good history match for the total flooding. Validation of these models by drawing the history match of water cut and oil recovery factor data at carbonate core sample is shown in Figure 19. Table 6 shows the all parameters to achieve date matching using CMG software.

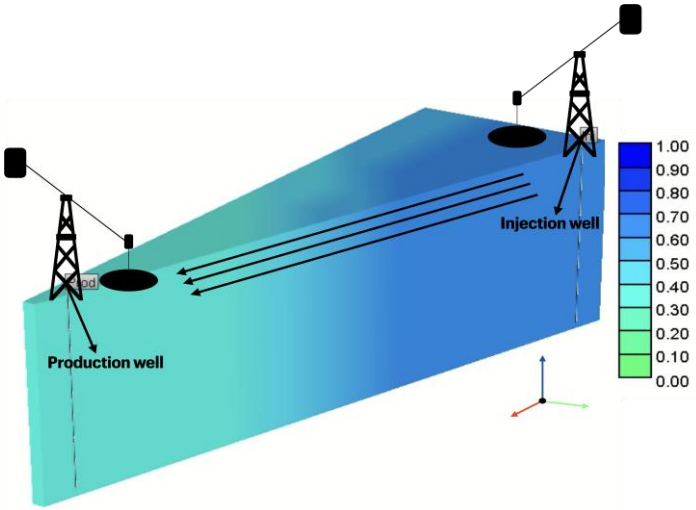


Figure 17. 3D view of the injection and production well's locations.

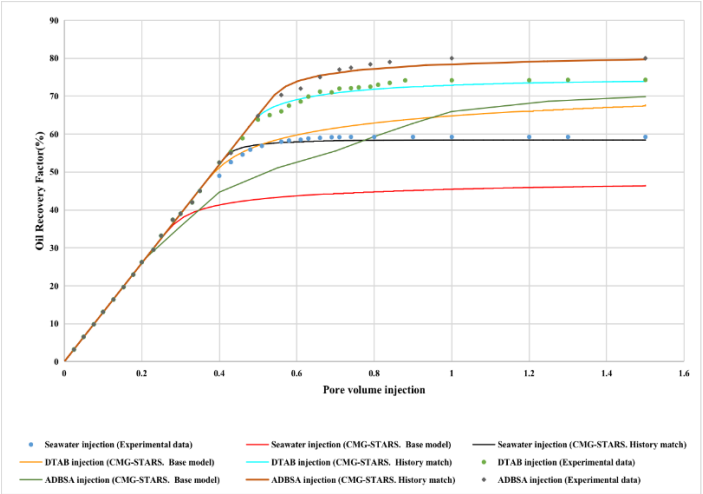


Figure 18. History matching of the experimental and simulation oil recovery Factor.

Table 6. all parameters for history matching.

Parameters	Seawater Injection	CTAB Surfactant	ADBSA Surfactant
Swcon (%)	0.23	0.23	0.23
Soirr (%)	0.32	0.2	0.16
Kro	0.87	0.87	0.87
Krw	0.34	0.62	0.8
Nw	4	3	5
No	1.2	1.3	1.1

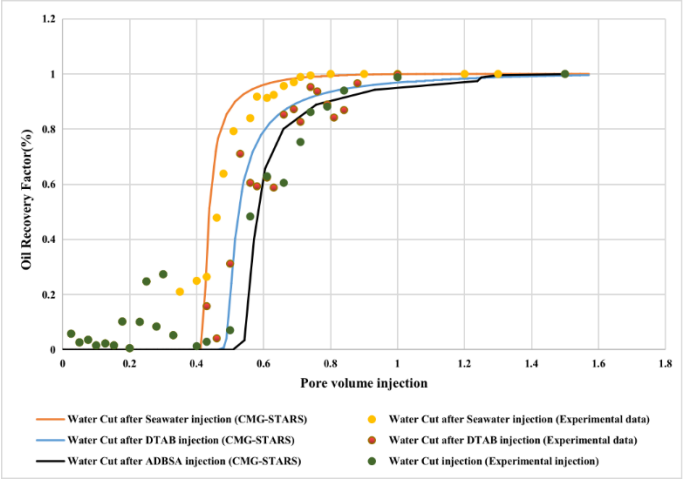


Figure 19. Water cut profiles solutions.

4. Conclusions

A) The cross point of oil and water relative permeability curves increased to higher value when surfactants is injected in all correlation and methods. This cross point occurs in saturation of 67% for water injection, 78% for DTAB injection and 83% for ADBSA injection. It shows that the rock move to more water-wet (Jones and Roszelle method).

B) As surfactant was injected instead of water, the relative permeability of oil in a certain saturation was increased. Relative permeability of oil in "ADBSA injection" was more than permeability of oil in "DTAB injection". This enhancement of oil permeability shows that when surfactant was injected instead of water, surfactant was placed between layers of oil, water and rocks and by changing of wettability caused oil was moved easier and faster and a greater amount of oil was extracted.

C) The contact angle between water drop and surface of the rock was 150 degree when the rock saturated with water, 87 degrees when it saturated with DTAB surfactant and when it saturated with ADBSA the contact angle was 60 degrees. That show surfactants was changed the wettability of the rock and the rock was more water-wet for "ADBSA surfactant", "DTAB surfactant" and "water", respectively.

D) When the surfactants were injected and changing the wettability of rock to more water-wet it caused the residual oil saturation was reduced. Residual oil saturation was reduced from 31 percent for water injection to 19 and 15 percent by injection of DTAB and ADBSA surfactant, respectively.

E) As shown in figure 4-11, "water break through" was happened later, when surfactants were injected instead of water. In comparison to DTAB injection "water break through" was happened later in ADBSA injection.

F) In water injection amount of oil recovery was 59 percent. But when DTAB is injected recovery of oil increased to 74 percent. Most oil recovery was seen when ADBSA was injected by 80 percent.

Credit Authorship Contribution Statement

Farhad Fallahi, Ghasem Zargar, Mohammad Ali Takasi, Fatemeh Ozar Asl, Siamak Moradi: Conceptualization, Investigation, Resources, Writing - Original Draft. Abbas Khaksar Manshad: Conceptualization, Supervision, Project administration, and Writing - Review & Editing.

Conflicts of Interest

The authors declare that they do not have any personal or financial conflicts of interest.

References

[1] D. W. Green, G. P. Willhite, Enhanced Oil Recovery. *Textbook series*, SPE, Vol. 6, Richardson, TX, 1998.

[2] J. R. Fanchi, Principles of Applied Reservoir Simulation, *Gulf Professional Publishing*, 2001.

[3] A. Roustaei, Investigating the Effect of Polysilicon Nano Powders in Waterflooding. *M.Sc. Thesis, Petroleum University of Technology, Abadan Faculty of Petroleum Engineering*, Abadan, Iran, 2012.

[4] ARI: Basin Oriented Strategies for CO_2 Enhanced Oil Recovery: Onshore Gulf Coast, *Prepared for U.S. Department of energy office of Fossil Energy – Office of Oil and Natural Gas by Advanced Resources International*, February, 2006.

[5] Schramm, L. Laurier, N. Elaine G. D. Marangoni, Surfactants and Their Applications, *Physical Chemistry and Chemical Physics Research, Section* 3, 2003, Vol. 99, 3-48.

[6] A. K. Abdulla, Impact of Wettability Alteration on Recovery Factor. *SPE Conference Paper, SPE/DGS Saudi Arabia Section Technical Symposium and Exhibition, Al-Khobar, Saudi Arabia*, 15-18 May, 2011.

[7] Ayirala, C. Subhash, Surfactant-induced relative permeability modifications for oil recovery enhancement. *PhD diss., IIT, Kharagpur, India*, 2002.